ISBN: 978-3-95450-204-2 ISSN: 2673-5350 doi:10.18429/JACoW-IBIC2019-TUA002

BEAM-LOSS DETECTION FOR LCLS-II*

Alan S. Fisher†, Christine I. Clarke, Bryce T. Jacobson, Ruslan Kadyrov,
Evan Rodriguez, Leonid Sapozhnikov, and James J. Welch
SLAC National Accelerator Laboratory, Menlo Park, California 94025, USA

Abstract

SLAC is now installing LCLS-II, a superconducting electron linac driven by continuous RF at 1.3 GHz. The 4-GeV, 120-kW beam has a 1-MHz maximum rate and can be switched pulse-by-pulse to either of two undulators, to generate hard and soft x rays. Two detector types measure beam losses. Point beam-loss monitors (PBLMs) set limits at critical loss points: septa, beam stoppers and dumps, halo collimators, protection collimators (which normally receive no loss), and zones with weak shielding. PBLMs are generally single-crystal diamond detectors, except at the gun, where a scintillator on a PMT is more sensitive to the low-energy (1 MeV) beam. Long beam-loss monitors (LBLMs) use 200-m lengths of radiation-hard optical fiber, each coupled to a PMT, to capture Cherenkov light from loss showers. LBLMs protect the entire 4-km path from gun to beam dump and locate loss points. In most regions two fibers provide redundancy and view the beam from different angles. Loss signals are integrated with a 500-ms time constant and compared to a threshold; if exceeded, the beam is stopped within 0.2 ms. We report on our extensive tests of the detectors and the front-end signal processing.

INTRODUCTION

SLAC has removed the first km of its 3-km copper electron linac, completely emptying this part of the tunnel and the Klystron Gallery above it for the first time since construction in the 1960s. Half the cryomodules of the new LCLS-II superconducting-RF (SRF) linac are now in the tunnel. In addition, two variable-gap undulators, for hard and soft x rays are replacing the fixed-gap LCLS undulator.

The superconducting linac, driven with continuous-wave (CW) 1.3-GHz RF, will produce 4-GeV bunches with variable spacing at rates of up to 1 MHz. The new machine raises the maximum beam power from 500 W to 120 kW. An 8-GeV upgrade will later double this power. The need to prevent damaging beam loss has grown proportionately.

Previous Beam-Loss Detectors

Beam-loss detection at SLAC has long depended on gas-filled ionization chambers. "Protection ionization chambers" (PICs) are point beam-loss monitors (PBLMs), placed at likely loss locations such as collimators. Long beam-loss monitors (LBLMs) detect losses over tens of meters, using "long ionization chambers" (LIONs), which are hollow gas-dielectric (Heliax) coaxial cables. Because the ion transit through both types is slow, 1 to 5 ms, ions will accumulate during high-loss bursts from a high-rate beam. As presented previously [1], the resulting space charge can screen the bias field inside the detector and suppress its response. This paper reports on the faster alternatives planned for LCLS-II [2], discussing both the design considerations and the testing necessary to gain approval for a new safety system.

BCS, MPS, and Diagnostics

The new loss detectors avoid past duplication by simultaneously serving three functions [2]: as inputs to the Beam Containment and Machine Protection Systems (BCS and MPS), and as beam diagnostics.

The BCS halts the beam if the loss level might harm people or safety devices. Because it requires robust and simple signal processing, with no knowledge of bunch timing and no software, loss signals are passively integrated on a capacitor with a 500-ms time constant. If this capacitor voltage exceeds a threshold, a shut-off command is issued.

The MPS is allowed greater flexibility to avoid damage from losses: it can trip the beam off or reduce its repetition rate, and recovers faster from trips. It shares the BCS time constant but with a lower trip threshold. A buffered copy of the integrated BCS signal is passed to the MPS.

Finally, the high-frequency component of the LBLM output will be digitized at 370 MHz and used as a diagnostic waveform, for beam-loss localization and for beam-profile measurements with fast wire scanners. The arrival time of a loss peak at the digitizer relative to the arrival of the electron bunch in the same region indicates the position of the loss. During a wire scan, software extracts the loss signal from the waveform and correlates it with the wire position to determine the bunch profile, without need for a dedicated detector. The software provides three sampling windows, configurable in width and delay, to numerically integrate loss peaks and subtract pedestal.

LONG BEAM-LOSS MONITORS

In place of LIONs, LCLS-II will use optical fibers as LBLMs. A loss shower passing through a fiber emits Cherenkov light, a portion of which is captured in a fiber mode and carried to a photomultiplier (PMT) at one end. For sensitivity, each fiber is relatively thick—with diameters of 600, 660, and 710 μm for the core, cladding, and buffer, respectively—and is encased in a 2-mm jacket of black polyurethane, for protection and opacity. The fiber, type FBP-600660710 from the Polymicro division of Molex, uses a special, radiation-resistant quartz. This and related types were subjected to extensive tests of radiation hardness for use in the end cap of the CMS detector on the LHC at CERN [3-5]. The FPB type was found to be superior, especially for red wavelengths around 700 nm.

* SLAC is supported by the U.S. Department of Energy, Office of Science, under contract DE-AC02-76SF00515.
† email address afisher@slac.stanford.edu

ISBN: 978-3-95450-204-2 ISSN: 2673-5350 doi:10.18429/JACoW-IBIC2019-TUA002

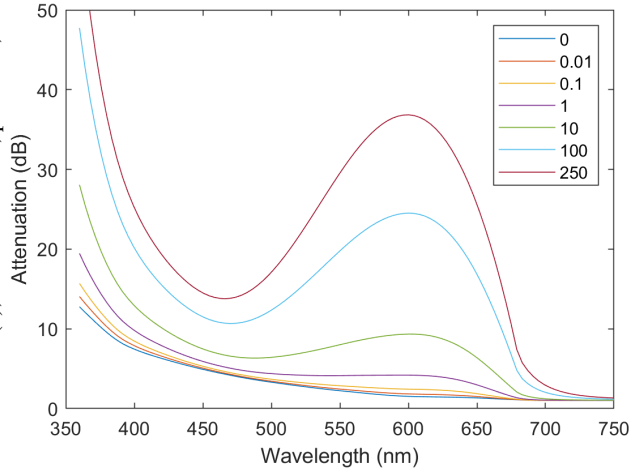

Figure 1: Radiation-induced attenuation in a 200-m fiber irradiated over 10 m, for various doses in kGy.

A distance of 4 km must be protected, from gun to beam dump, in most places using two fibers both for redundancy and also for different viewing angles. This distance is subdivided into lengths of roughly 200 m, with variations to span functional sections, such as the injector or the L2 linac between the first and second bunch compressors.

Fiber Attenuation

A reasonably calibrated basis for setting the trip threshold requires comparable signals from losses near the two ends of the fiber. Our criterion is that these signals must not differ by more than 3 dB (a factor of 2), despite fiber attenuation after irradiation during several years of use. Even without radiation, the criterion restricts the wavelength to $\lambda > 510$ nm due to the inherent attenuation of blue light in a 200-m fiber (lowest curve of Fig. 1). An optical filter at the PMT window removes these shorter wavelengths.

However, a longer cutoff is needed to include the wavelength dependence of radiation-induced attenuation. This effect was parameterized in [4] for a similar Polymicro quartz fiber, type FVP, which is shown in [5] to be somewhat worse in the red than FBP. The expression in [4] then allows a conservative calculation of fiber attenuation due to a steady irradiation of 10 of its 200 m by beam loss at a level that does not trip the beam (curves of Fig. 1). Attenuation at 700 nm remains small and meets the 3-dB criterion.

The relative PMT signal can be found by integrating over the Cherenkov emission, the fiber transmission, and the PMT quantum efficiency (QE). In a low-radiation area, it can be helpful to gain signal strength by extending the cutoff wavelength toward the green. For example, the linac-to-undulator (LTU) transfer hall runs above ground in a concrete bunker that was sufficient at 120 Hz but offers only moderate shielding for the high-rate beam. Adequate protection for people outside demands a low trip threshold inside. A fiber dose limit of 1 kGy, which allows several years of use in this low-radiation zone, can satisfy the 3-dB criterion with a filter cutoff of 555 nm. The larger signal improves the measurement near this low threshold. In contrast, a fiber in the linac, where the threshold is higher, is also expected to receive a higher dose. There the filter cutoff is 675 nm, corresponding to 100 kGy.

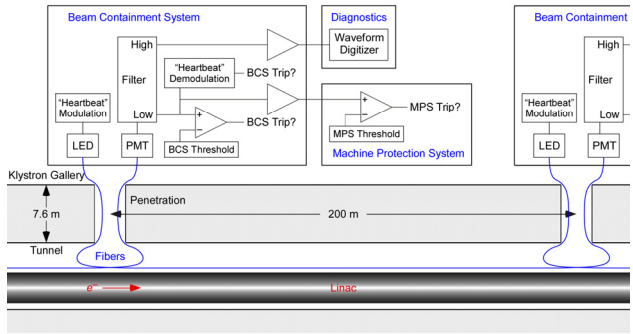

Figure 2: Typical fiber layout in the linac tunnel, including the PMT at the downstream end and the "heartbeat" LED at the upstream end. The splitter that provides a signal for three functions is indicated.

Photomultiplier Selection and Fiber Layout

Most photocathodes are insensitive at 700 nm. We have chosen the Hamamatsu H7422P-40, a PMT with a GaAsP cathode that has a QE of 30% at this wavelength. This sensitivity to red photons comes at the cost of higher PMT dark current, which could limit the ability to measure small but potentially CW losses of structure dark current from the electron gun or SRF cavities. However, PMT dark current is thermal, dropping by a factor of 2 for every 5°C of cooling until this benefit levels off at 0°C. The housing of this PMT includes a Peltier cooler that maintains an operating temperature of 0°C.

Both ends of the fiber up come up from the tunnel to the Klystron Gallery, about 11 m above the linac. One end runs to a rack with an LBLM chassis containing a PMT, with its entrance window covered by a suitable optical filter and an SMA-905 fiber connector. Figure 2 illustrates the layout.

The other end of the fiber goes to a similar chassis, where it connects to an SMA-905 containing an LED emitting at a wavelength just within the edge of the filter's passband. The LED provides a "heartbeat", a continuous test of the fiber system. A small sinusoidal current is driven in the LED at 0.8 Hz, modulating the PMT signal. The low frequency passes through the integrator to a digital signal processor (DSP), which detects it at a very low level using an algorithm like that of a digital lock-in amplifier. Synchronization between the drive and the detection, 200 m apart, is ensured by counting cycles of the 60-Hz AC power line: 0.8 Hz = 60 Hz/75. A missing heartbeat—indicating a failure of the fiber, the PMT, its power supply, or the electronics—leads to a BCS trip. Such a narrow-band filter is slow, requiring over a minute to settle after the power comes on and a similar time to trip if the signal is lost, but this is sufficiently fast for BCS.

The control system archives the detected heartbeat amplitude, so that any gradual degradation of the fiber transmission can be tracked. If after some years a fiber needs replacement, it can be done quickly, without entering the tunnel and without halting the beam. "Ducts" of polyeth-

ISBN: 978-3-95450-204-2 ISSN: 2673-5350 doi:10.18429/JACoW-IBIC2019-TUA002

ylene tubing with a 6-mm inner diameter are being installed along the fiber routes (first in the linac area, since access will not be possible once the cryostats are in place). Each fiber, forced by pressure from compressed nitrogen and guided through a special fixture, will be blown within minutes through its duct, from a Gallery rack at one end of the path to the rack at the other end. After attaching SMA connectors to the ends, the new fiber is ready for use.

Modeling and Testing

The geometry for capturing Cherenkov light in a fiber is complex. The Cherenkov cone emitted by a particle from a loss shower is at nearly 45° to the direction of travel. Only part of the cone falls within the capture angle of about 9° to the fiber axis. Capture is then most effective where the particle enters at nearly to 45° to the axis, which mostly happens near the loss source, but showering and screening by intervening objects can alter the signal. We have modeled this process with an extension [6] to FLUKA.

Tests with 100 m of fiber along the LCLS linac and 150 m in the beam switchyard (BSY) downstream identified loss locations within about 3 m. The BSY fiber had identical PMTs at both ends, to compare signals from light captured in the forward and backward directions. If losses occur at two points, the time separation of the peaks at the backward PMT is 5 times greater than at the forward PMT, due to the travel times of the shower particles and the captured light. Wider separation helps somewhat with loss localization, but zooming in on the forward signal allows comparable accuracy, limited by the PMT rise time and digitizer bandwidth. The forward PMT has a greater advantage: most loss is forward directed, producing a signal that was four times larger in our test. As Fig. 2 shows, each of our PMTs will be at the downstream end of its fiber.

POINT BEAM-LOSS MONITORS

In place of PICs, LCLS-II will use diamond-based detectors as PBLMs. A loss shower passing through a thin diamond creates electron-hole pairs, drawn by a bias voltage to metal electrodes plated on the opposite faces. The diamond resembles a solid-state ionization chamber, but with the important difference that both electrons and holes take only a few ns to reach the electrodes: no pile-up of ions can happen. Unlike an LBLM, loss localization is not important for a PBLM, since each is placed near a loss point.

We tested three types of diamond detectors, all originally developed for CERN and made by Cividec: the single-crystal B1, the polycrystalline B2, and the high-radiation B4. Both the B1 and B2 have a wide dynamic range, responding to the passage of 1 to 10^6 particles (at the ionization minimum, MIPs). The B2 has the benefit of a volume that is four times larger. However, we observed a slow tail when the loss stopped. In Fig. 3, about 1 W of the LCLS beam was scraped on a collimator monitored by a B1 and B2, as the beam rate was switched between 0 and 120 Hz. The B2 exhibited dual time constants, initially 2 s followed by 18 s. This effect is attributed to charge traps at domain boundaries. Because no tails are seen with the single-crystal B1, we have chosen this type for LCLS-II. The B4 is

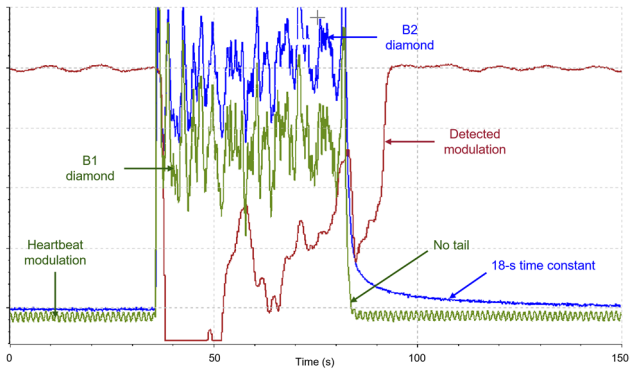

Figure 3: Cividec single-crystal B1 (green) and a polycrystalline B2 (blue) detectors measure a 1-W loss on an LCLS collimator as the beam rate was toggled between 0 and 120 Hz. The B2 exhibits a long decay tail. The red signal is the heartbeat amplitude detected by the DSP.

not well suited to our purpose, since it has a low sensitivity intended to avoid saturation in a high-radiation environment. It also shows an even longer decay tail and a slower rise, as its traps empty and refill.

The diamond also has a continuous heartbeat test, accomplished by modulating its bias voltage at 0.8 Hz. The small capacitance of the diamond is sufficient to provide a current that passes through the 500-ms filter for detection by a lock-in implemented on a DSP. Figure 3 shows the first test, with a noticeable sinusoidal amplitude seen on the B1. Further improvements to the filter algorithm now provide a robust detection of the heartbeat using a modulation that is no longer visible on this scale.

Cables

Unlike an LBLM, a diamond requires two long cables to carry the bias and the output current, typically a few nA at the MPS threshold, to the rack outside the tunnel. Recall that a passive *RC* filter receives this current. The capacitance (including cable capacitance) is chosen to give a suitable voltage for the integrated loss signal at the trip level. The resistor gives the desired time constant; the PBLMs use 15 MΩ. This must be well below the leakage resistance through the dielectric of the coaxial signal cable over its length (50 to 150 m), a specification that manufacturers do not provide. We tested several long cables by charging them up (within their voltage specification) and measuring the resistance of the dielectric, using a picoammeter with a 10-fA resolution. The resistance was sufficiently high. Afterward, we disconnected and discharged the cables with a 50-Ω termination. To our great surprise, when we reconnected one end of the cable to the meter and left the other open, the meter registered a DC current of as much as 1 nA. Discharging for minutes, then hours, and finally a few days, did not help: the current resumed when the cable was reconnected to the meter. A voltmeter read a few mV, consistent with the picoammeter. The engineering experts at the cable manufacturer had no explanation, but sent us several types of cable to test. (Double-shielded cable was preferred to avoid pick-up from kickers.) Ultimately, we do

ISBN: 978-3-95450-204-2 ISSN: 2673-5350 doi:10.18429/JACoW-IBIC2019-TUA002

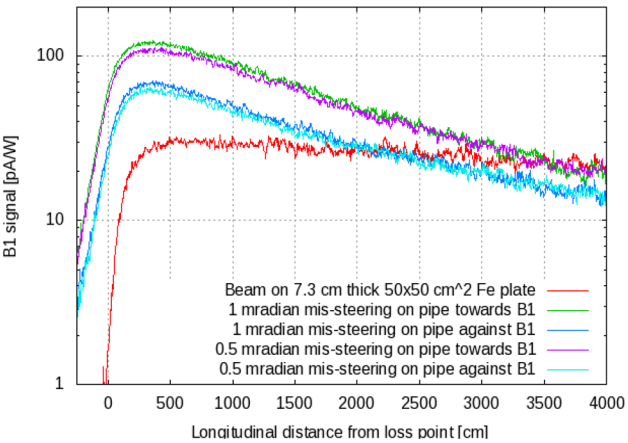

Figure 4: Current (pA) from a B1 diamond placed 2 m transversely from the beampipe, as a function of the longitudinal distance from a 1-W beam loss on a protection collimator (red) or a 1.5-mm-thick stainless-steel beampipe.

not understand this behavior but found some variants of RG-223 that do not exhibit it.

Modeling and Testing

PBLMs primarily protect collimators, stoppers and dumps from excessive power. Each halo collimator has one as part of MPS. Halo loss is expected, but excessive power may result from incorrect steering of the beam or positioning of a collimator jaw. Other PBLMs measure radiation from protection collimators, for BCS. These do not normally receive beam. In many locations after the linac tunnel, if a beam passes through the thin beampipe wall, a protection collimator—a barrier typically 50-cm square and 4 radiation-lengths thick (73 mm of steel), surrounding the beampipe—spreads out the beam to prevent a direct hit downstream by a thin beam.

Another FLUKA extension [6] uses the fluences and energies of the various shower particles to calculate the diamond signal, based on proprietary response data supplied by Cividec. These simulations [7] show that a loss on a protection collimator produces a diamond signal that is nearly constant over a longitudinal distance of over 20 m, when measured at a transverse distance of 1.5 to 2 m from the beampipe (Fig. 4). Areas, rather than individual protection collimators, can be covered by locating one diamond every 20 m between beamlines. With many such collimators on adjacent beamlines in the BSY and LTU, this scheme offers a considerable economy in the number of detectors. In an test of this effect in End Station A at SLAC, a beam hit a 16-cm-square, 80-mm-thick iron block. A B1 diamond was placed 166 cm to the side, suspended from the shielding wall on a motorized clothesline, and moved downstream of the block from −1 to +17 m. The signal was not as flat with distance as expected, but a more detailed analysis, accounting for the smaller block width and screening by obstacles that could not be removed from the tunnel, found consistency with the modeling code.

Locations for the diamonds have been marked in the tunnel, and cable installation is underway. The diamonds have been received and tested with a ^{137}Cs source at the SLAC Radiation Test Facility.

Scintillators

The LCLS-II electron gun uses CW RF at 185.7 MHz, 1/7 of the linac frequency. The output energy is just under 1 MeV, low compared to the LCLS RF gun. For commissioning the gun and the first few meters of beamline, we installed a short fiber and two diamonds, but they are not expected to give more than a weak response at this energy. Consequently, two YAP scintillators (from Crytur) with PMTs have been installed, one near the gun exit and the other 1 m downstream, by the entrance window for photocathode laser light. Tests to date have only involved dark current, which was easily detected by the scintillator (but not by the diamonds mounted next to them, nor by the fiber). The loss can be shifted from one scintillator to the other with the focusing solenoid at the gun output. Photocurrent tests have just begun with a Cs_2Te photocathode.

SUMMARY

Instead of ionization devices for beam-loss protection, LCLS-II will use optical fibers as long beam-loss monitors and diamond-based sensors as point beam-loss monitors. Both types have been extensively tested with SLAC beams, primarily at LCLS, but also at End Station A and SPEAR3.

More information about the signal processing will be presented at an upcoming conference [8].

REFERENCES

[1] A. S. Fisher, R. C. Field, and L. Y. Nicolas, "Evaluating beam-loss detectors for LCLS-2", in *Proc. IBIC'16*, Barcelona, Spain, Sep. 2016, pp. 678-681. doi:10.18429/JACoW-IBIC2016-WEPG23

[2] A. S. Fisher *et al.*, "Beam containment and machine protection for LCLS-2", in *Proc. IBIC'17*, Grand Rapids, MI, USA, Aug. 2017, pp. 478-481. doi:10.18429/JACoW-IBIC2017-TH1AB2

[3] I. Dumanoglu et al., "Radiation-hardness studies of high OH^- content quartz fibres irradiated with 500-MeV electrons," *Nucl. Instrum. Methods A*, vol. 490, p. 444, 2002.

[4] K. Cankoçak et al., "Radiation-hardness measurements of high OH^- content quartz fibres irradiated with 24-GeV protons up to 1.25 Grad," *Nucl. Instrum. Methods A*, vol. 585, p. 20, 2008. doi:10.1016/j.nima.2007.10.024

[5] P. G. Bruecken et al., "Results from *post situ* quartz fiber neutron irradiations", CMS Internal Note CMS-IN-2006/000, 2006.

[6] M. Santana-Leitner *et al.*, "Monte Carlo optimization of fast beam loss monitors for LCLS-II", *Proc. IPAC'19*, Melbourne, Australia, May 2019, pp. 4066-4069. doi:10.18429/JACoW-IPAC2019-THPRB102

[7] M. Santana-Leitner and T. Liang, "Expected signal at monocrystalline diamond detectors for canonical radiation sources at LCLS-II", SLAC Radiation Physics Note RP-18-21, Aug. 2018.

[8] Ruslan Kadyrov *et al.*, "Electronics for LCLS-II beam containment system loss monitors", to be published in *Proc. ICAPLEPS'19*, New York, NY, USA, Oct. 2019.